

OPARC: Optimal and Precise Array Response Control Algorithm – Part I: Fundamentals

Xuejing Zhang, *Student Member, IEEE*, Zishu He, *Member, IEEE*, Xiang-Gen Xia, *Fellow, IEEE*, Bin Liao, *Senior Member, IEEE*, Xuepan Zhang, and Yue Yang, *Student Member, IEEE*

Abstract—In this paper, the problem of how to optimally and precisely control array response levels is addressed. By using the concept of the optimal weight vector from the adaptive array theory and adding virtual interferences one by one, the change rule of the optimal weight vector is found and a new formulation of the weight vector update is thus devised. Then, the issue of how to precisely control the response level of one single direction is investigated. More specifically, we assign a virtual interference to a direction such that the response level can be precisely controlled. Moreover, the parameters, such as, the interference-to-noise ratio (INR), can be figured out according to the desired level. Additionally, the parameter optimization is carried out to obtain the maximal array gain. The resulting scheme is called optimal and precise array response control (OPARC) in this paper. To understand it better, its properties are given, and its comparison with the existing accurate array response control (A²RC) algorithm is provided. Finally, simulation results are presented to verify the effectiveness and superiority of the proposed OPARC.

Index Terms—Array response control, adaptive array theory, array pattern synthesis, array signal processing.

I. INTRODUCTION

ARRAY antenna has been extensively applied in many fields, such as, radar, navigation and wireless communications [1]. It is known that the array pattern design is of significant importance to enhance system performance. For instance, in radar systems, it is desirable to mitigate returns from interfering signals, by designing a scheme which results in nulls at directions of interferences. In some communication systems, it is critical to shape multiple-beam patterns for multi-user reception. Additionally, synthesizing a pattern with broad mainlobe is beneficial to extend monitoring areas in satellite remote sensing. Generally speaking, array pattern can be designed either adaptively or non-adaptively. Determining the complex weights for array elements so as to achieve a desired beampattern is known as array pattern synthesis. With regard to this problem, it is expected to find weights that satisfy a set of specifications on a given beampattern, in a data-independent or nonadaptive manner.

X. Zhang, Z. He and Y. Yang are with the University of Electronic Science and Technology of China, Chengdu 611731, China (e-mail: xjzhang7@163.com; zshe@uestc.edu.cn; yueyang@std.uestc.edu.cn).

X. Zhang and X.-G. Xia are with the Department of Electrical and Computer Engineering, University of Delaware, Newark, DE 19716, USA (e-mail: xjzhang@udel.edu; xxia@ee.udel.edu).

B. Liao is with College of Information Engineering, Shenzhen University, Shenzhen 518060, China (e-mail: binliao@szu.edu.cn).

X. P. Zhang is with Qian Xuesen Lab of Space Technology, Beijing 100094, China (e-mail: zhangxuepan@qxslab.cn).

Over the past several decades, a great number of pattern synthesis approaches have been proposed, see, e.g., [2]–[14]. Particularly, in [12], an iterative sampling method is utilized to make the sidelobe peaks conform to a specified shape within a given tolerance. For sidelobe control in cylindrical arrays, an artificially created noise source environment can be utilized [13]. For a circular ring array, a symmetrical pattern with low sidelobes is achieved in [14] by adopting a field-synthesis technique. Note that although the solutions in [12]–[14] are able to control sidelobes for arrays with some particular configurations, they cannot be straightforwardly extended to general geometries. On the contrary, the accurate array response control (A²RC) approach [15] provides a simple and effective manner to accurately control array response level of arbitrary arrays. Since the A²RC approach deals with the response control of a single direction, more recently, a multi-point accurate array response control (MA²RC) method has been developed in [16] to flexibly adjust array responses of multiple points. However, a satisfactory performance cannot be always guaranteed in either [15] or [16] due to the empirical solution adopted in this kind of approaches.

These shortcomings of the existing approaches motivate us to have an innovative method to precisely, flexibly and optimally control the response level. To do so, we first investigate how the optimal weight vector in the adaptive array theory changes along with the increase of the number of interferences. Then, a new scheme for weight vector update is developed and further exploited to realize the precise array response control. Furthermore, a parameter optimization mechanism is proposed by maximizing the array gain [17]. It is shown that, the proposed optimal and precise array response control (OPARC) approach is capable of precisely and flexibly controlling the response level of an arbitrary array. Furthermore, its optimality (in the sense of array gain) can be well guaranteed. In this paper, the proposed OPARC scheme is developed by exploiting the interference-to-noise ratio (INR).

It should be mentioned that this paper focuses on the main concepts and fundamentals of the OPARC scheme, while the extensions and applications (such as pattern synthesis and quiescent pattern control [18]) will be carried out in the companion paper [19]. The rest of the paper is organized as follows. Our proposed OPARC algorithm is presented in Section II. Further insights into OPARC are presented in Section III to provide more useful and interesting properties. In Section IV, comparisons between OPARC and the existing A²RC are presented. Representative simulations are conducted in Section V and conclusions are drawn in Section VI.

Notations: We use bold upper-case and lower-case letters to represent matrices and vectors, respectively. In particular, we use \mathbf{I} , $\mathbf{1}$ and $\mathbf{0}$ to denote the identity matrix, the all-one vector and the all-zero vector, respectively. $j \triangleq \sqrt{-1}$. $(\cdot)^T$, $(\cdot)^*$ and $(\cdot)^H$ stand for the transpose, complex conjugate and Hermitian transpose, respectively. $|\cdot|$ denotes the absolute value and $\|\cdot\|_2$ denotes the l_2 norm. We use $\mathbf{H}(i, l)$ to stand for the element at the i th row and l th column of matrix \mathbf{H} . $\Re(\cdot)$ and $\Im(\cdot)$ denote the real and imaginary parts, respectively. $\det(\cdot)$ is the determinant of a matrix. The sign function is denoted by $\text{sign}(\cdot)$. \oslash represents the element-wise division operator. We use $\text{diag}(\cdot)$ to return a column vector composed of the diagonal elements of a matrix, and use $\text{Diag}(\cdot)$ to stand for the diagonal matrix with the components of the input vector as the diagonal elements. Finally, \mathbb{R} and \mathbb{C} denote the sets of all real and all complex numbers, respectively, and \mathbb{S}_{++}^N denotes the set of $N \times N$ positive definite matrices.

II. OPARC ALGORITHM

In order to present our proposed OPARC algorithm, we first briefly recall the adaptive array theory.

A. Adaptive Array Theory

Consider an array of N elements and assume that the noise is white and the interferences are independent with each other. To suppress the unwanted interferences and noise, the optimal adaptive beamformer weight vector \mathbf{w} steering to the direction θ_0 can be obtained by maximizing the output signal-to-interference-plus-noise ratio (SINR) defined as

$$\text{SINR} = \frac{\sigma_s^2 |\mathbf{w}^H \mathbf{a}(\theta_0)|^2}{\mathbf{w}^H \mathbf{R}_{n+i} \mathbf{w}} \quad (1)$$

where σ_s^2 stands for the signal power, \mathbf{R}_{n+i} denotes the $N \times N$ noise-plus-interference covariance matrix and $\mathbf{a}(\theta_0)$ represents the signal steering vector. More exactly, for a given θ , we have

$$\mathbf{a}(\theta) = [g_1(\theta)e^{-j\omega\tau_1(\theta)}, \dots, g_N(\theta)e^{-j\omega\tau_N(\theta)}]^T \quad (2)$$

where $g_n(\theta)$ denotes the pattern of the n th element, $\tau_n(\theta)$ is the time-delay between the n th element and the reference point, $n = 1, \dots, N$, ω denotes the operating frequency.

It is known that the optimal weight vector \mathbf{w}_{opt} , which maximizes the SINR, is given by [17]

$$\mathbf{w}_{\text{opt}} = \alpha \mathbf{R}_{n+i}^{-1} \mathbf{a}(\theta_0) \quad (3)$$

where α is a normalization factor and does not affect the output SINR, and hence, will be omitted in the sequel.

Note that the above SINR can be expressed as $G \cdot \sigma_s^2 / \sigma_n^2$, where G is defined as

$$G = \frac{|\mathbf{w}^H \mathbf{a}(\theta_0)|^2}{\mathbf{w}^H \mathbf{T}_{n+i} \mathbf{w}} \quad (4)$$

with $\mathbf{T}_{n+i} \triangleq \mathbf{R}_{n+i} / \sigma_n^2$ standing for the normalized noise-plus-interference covariance matrix, i.e.,

$$\mathbf{T}_{n+i} = \frac{\mathbf{R}_{n+i}}{\sigma_n^2} = \mathbf{I} + \sum_{\ell=1}^k \beta_\ell \mathbf{a}(\theta_\ell) \mathbf{a}^H(\theta_\ell) \quad (5)$$

where $\beta_\ell \triangleq \sigma_\ell^2 / \sigma_n^2$ denotes the interference-to-noise ratio (INR), k is the number of interferences, $\mathbf{a}(\theta_\ell)$ is the steering vector of the ℓ th interference, σ_n^2 and σ_ℓ^2 stand for the noise and interference powers, respectively.

Note that G represents the amplification factor of the input signal-to-noise ratio (SNR) σ_s^2 / σ_n^2 , and therefore, is termed as the array gain [17]. As a result, the criterion of array gain G maximization is adopted to achieve the optimal weight vector.

B. Update of the Optimal Weight Vector

It can be seen from (3)–(5) that the optimal weight vector \mathbf{w}_{opt} depends on \mathbf{R}_{n+i} or \mathbf{T}_{n+i} , which is not available for the following data-independent array response control: for a given steering vector $\mathbf{a}(\theta)$ in (2) and a beam axis θ_0 , design a weight vector \mathbf{w} such that the normalized array response $L(\theta, \theta_0) \triangleq |\mathbf{w}^H \mathbf{a}(\theta)|^2 / |\mathbf{w}^H \mathbf{a}(\theta_0)|^2$ meets some specific requirements. In this paper, we are interested in the requirements of array response levels, i.e., finding weight vectors such that the array responses at a given set of angles are equal to a set of prescribed values. Our basic idea is to construct a virtual normalized noise-plus-interference covariance matrix (VCM), denoted as \mathbf{T}_k , to achieve the given response control task. Note that since the VCM \mathbf{T}_k to be determined is not produced by real data, it may not have any physical meaning. Moreover, it can be neither positive definite nor Hermitian (its rationality will be discussed later). By making use of the VCM, the data-dependent adaptive array theory can be applied to the data-independent situation considered in this paper. This allows us to optimally update the weight vector $\mathbf{w}_{k-1, \text{opt}} = \mathbf{T}_{k-1}^{-1} \mathbf{a}(\theta_0)$ to $\mathbf{w}_{k, \text{opt}}$ such that a desired response level ρ_k at θ_k can be achieved by assigning an appropriate virtual interference. Thus, the problem we concern here is to figure out the characteristics, e.g., INR, of the virtual interference.

We use induction to describe the problem and the algorithm below. Suppose that the response levels of the $k-1$ directions have been successively controlled by adding $k-1$ virtual interferences. Meanwhile, the corresponding VCM is denoted as \mathbf{T}_{k-1} . For a given θ_k and its desired level ρ_k , we can assign the k th virtual interference coming from θ_k by designing its INR (i.e., β_k). To find out β_k , from (5) we notice that the VCM can be updated as

$$\mathbf{T}_k = \mathbf{T}_{k-1} + \beta_k \mathbf{a}(\theta_k) \mathbf{a}^H(\theta_k). \quad (6)$$

Using the Woodbury Lemma [20], we have

$$\mathbf{T}_k^{-1} = \mathbf{T}_{k-1}^{-1} - \frac{\beta_k \mathbf{T}_{k-1}^{-1} \mathbf{a}(\theta_k) \mathbf{a}^H(\theta_k) \mathbf{T}_{k-1}^{-1}}{1 + \beta_k \mathbf{a}^H(\theta_k) \mathbf{T}_{k-1}^{-1} \mathbf{a}(\theta_k)}. \quad (7)$$

Accordingly, the optimal weight vector is given by $\mathbf{w}_{k, \text{opt}} = \mathbf{T}_k^{-1} \mathbf{a}(\theta_0)$. Recalling (3) and (7), we can express $\mathbf{w}_{k, \text{opt}}$ as

$$\mathbf{w}_{k, \text{opt}} = \mathbf{w}_{k-1, \text{opt}} + \gamma_k \mathbf{T}_{k-1}^{-1} \mathbf{a}(\theta_k) \quad (8)$$

where $\mathbf{w}_{k-1, \text{opt}} = \mathbf{T}_{k-1}^{-1} \mathbf{a}(\theta_0)$ denotes the previous optimal weight vector and γ_k is given by

$$\gamma_k = -\frac{\beta_k \mathbf{a}^H(\theta_k) \mathbf{T}_{k-1}^{-1} \mathbf{a}(\theta_0)}{1 + \beta_k \mathbf{a}^H(\theta_k) \mathbf{T}_{k-1}^{-1} \mathbf{a}(\theta_k)} \triangleq \Psi_k(\beta_k) \quad (9)$$

with $\Psi_k(\cdot)$ denoting a mapping from β_k to γ_k .

Note that the solution in (8)–(9) gives the optimal solution for maximizing the SINR, which may not meet the response level ρ_k at θ_k . In order to meet this response level requirement, we next consider the following questions first. Given the previous weight vector $\mathbf{w}_{k-1,\text{opt}} = \mathbf{T}_{k-1}^{-1}\mathbf{a}(\theta_0)$, does there exist γ_k (or equivalently β_k) such that the response level at θ_k is precisely ρ_k ? and what value it should be if it exists? To do so, we reformulate the weight vector as

$$\mathbf{w}_k = \mathbf{w}_{k-1} + \gamma_k \mathbf{v}_k \quad (10)$$

where the subscript $(\cdot)_{\text{opt}}$ is omitted for notational simplicity and \mathbf{v}_k is defined as

$$\mathbf{v}_k \triangleq \mathbf{T}_{k-1}^{-1}\mathbf{a}(\theta_k). \quad (11)$$

Mathematically, the problem of finding γ_k such that the array response level at θ_k is ρ_k can be written as

$$L(\theta_k, \theta_0) = |\mathbf{w}_k^H \mathbf{a}(\theta_k)|^2 / |\mathbf{w}_k^H \mathbf{a}(\theta_0)|^2 = \rho_k \quad (12)$$

where the desired array response level satisfies $\rho_k \leq 1$. The combination of (10) and (12) yields

$$\mathbf{z}_k^H \mathbf{H}_k \mathbf{z}_k = 0 \quad (13)$$

where \mathbf{z}_k and \mathbf{H}_k are, respectively, defined as

$$\begin{aligned} \mathbf{z}_k &\triangleq [1 \ \gamma_k]^T \\ \mathbf{H}_k &\triangleq [\mathbf{w}_{k-1} \ \mathbf{v}_k]^H (\mathbf{a}(\theta_k)\mathbf{a}^H(\theta_k) - \rho_k \mathbf{a}(\theta_0)\mathbf{a}^H(\theta_0)) [\mathbf{w}_{k-1} \ \mathbf{v}_k]. \end{aligned} \quad (14)$$

By expanding (13) and (14), we immediately have the following proposition.

Proposition 1: Suppose that γ_k (i.e., the second entry of \mathbf{z}_k) satisfies (13), if $\mathbf{H}_k(2, 2) = 0$, it can be derived that the trajectory of $[\Re(\gamma_k) \ \Im(\gamma_k)]^T$ is a line as

$$\Re[\mathbf{H}_k(1, 2)]\Re(\gamma_k) - \Im[\mathbf{H}_k(1, 2)]\Im(\gamma_k) = -\mathbf{H}_k(1, 1)/2.$$

If $\mathbf{H}_k(2, 2) \neq 0$, the trajectory of $[\Re(\gamma_k) \ \Im(\gamma_k)]^T$ is a circle, denoted by \mathbb{C}_γ :

$$\mathbb{C}_\gamma = \left\{ [\Re(\gamma_k) \ \Im(\gamma_k)]^T \mid \left\| [\Re(\gamma_k) \ \Im(\gamma_k)]^T - \mathbf{c}_\gamma \right\|_2 = R_\gamma \right\}$$

with the center

$$\mathbf{c}_\gamma = \frac{1}{\mathbf{H}_k(2, 2)} \begin{bmatrix} -\Re[\mathbf{H}_k(1, 2)] \\ \Im[\mathbf{H}_k(1, 2)] \end{bmatrix} \quad (15)$$

and the radius

$$R_\gamma = \sqrt{-\det(\mathbf{H}_k)} / |\mathbf{H}_k(2, 2)|. \quad (16)$$

From this proposition, it is known that, given the previous weight vector $\mathbf{w}_{k-1} = \mathbf{T}_{k-1}^{-1}\mathbf{a}(\theta_0)$, there exist infinitely many solutions of γ_k to achieve a response level of ρ_k at θ_k . This implies that the response level at a certain direction can be precisely adjusted by assigning a virtual interference with properly designed INR parameter γ_k .

It is clear that $\mathbf{H}_k(2, 2) = 0$ is equivalent to

$$\rho_k = \frac{|(\mathbf{T}_{k-1}^{-1}\mathbf{a}(\theta_k))^H \mathbf{a}(\theta_k)|^2}{|(\mathbf{T}_{k-1}^{-1}\mathbf{a}(\theta_k))^H \mathbf{a}(\theta_0)|^2}. \quad (17)$$

In this case ρ_k is equal to the normalized power response at θ_k when the weight vector is $\mathbf{T}_{k-1}^{-1}\mathbf{a}(\theta_k)$, i.e., when the

beam pattern steers to the beam axis θ_k . Typically, a beam pattern reaches its maximum at the beam axis, i.e., we have $\rho_k > 1$ if $\theta_k \neq \theta_0$. This would contradict with the fact that $\rho_k \leq 1$. Hence, $\mathbf{H}_k(2, 2) = 0$ usually will not occur and in the sequel we only focus on the case of $\mathbf{H}_k(2, 2) \neq 0$, and from Proposition 2, the trajectory of $[\Re(\gamma_k) \ \Im(\gamma_k)]^T$ is a circle, as illustrated in Fig. 1. Then, the remaining question is among all these valid solutions of γ_k (or β_k), to meet the response level requirement, which one is to maximize the SINR or beam gain? We will study this question below.

C. Selection of γ_k and Update of the Weight Vector

The preceding problem can be formulated as the following constrained optimal and precise array response control (OPARC) problem:

$$\underset{\gamma_k}{\text{maximize}} \quad G_k \triangleq |\mathbf{w}_k^H \mathbf{a}(\theta_0)|^2 / |\mathbf{w}_k^H \mathbf{T}_k \mathbf{w}_k| \quad (18a)$$

$$\text{subject to} \quad L(\theta_k, \theta_0) = \rho_k \quad (18b)$$

$$\mathbf{w}_k = \mathbf{w}_{k-1} + \gamma_k \mathbf{T}_{k-1}^{-1}\mathbf{a}(\theta_k). \quad (18c)$$

From (18a), one can see that the desired weight vector is expected to provide the maximum array gain with some additional constraints. Moreover, in the above devised OPARC scheme, apart from the response level constraint (18b), we have also imposed constraint (18c) to make the resultant \mathbf{w}_k be a particular optimal weight vector in correspondence to assigning another interference at θ_k to the existing $k - 1$ interferences at directions $\theta_1, \dots, \theta_{k-1}$.

When γ_k satisfies (9), (18c) leads to $\mathbf{w}_k = \mathbf{T}_k^{-1}\mathbf{a}(\theta_0)$. In order to solve problem (18), we first substitute $\mathbf{w}_k = \mathbf{T}_k^{-1}\mathbf{a}(\theta_0)$ into the objective function and get $G_k = |\mathbf{a}^H(\theta_0)\mathbf{T}_k^{-H}\mathbf{a}(\theta_0)|$. Then, recalling (7) and (9), we can rewrite G_k as

$$\begin{aligned} G_k &= |\mathbf{a}^H(\theta_0)\mathbf{T}_{k-1}^{-1}\mathbf{a}(\theta_0) + \gamma_k \mathbf{a}^H(\theta_0)\mathbf{T}_{k-1}^{-1}\mathbf{a}(\theta_k)| \\ &= |\tilde{\xi}_c| \cdot |\xi_0/\tilde{\xi}_c + \gamma_k| \end{aligned} \quad (19)$$

where ξ_0 , ξ_k , ξ_c and $\tilde{\xi}_c$ are defined as

$$\xi_0 \triangleq \mathbf{a}^H(\theta_0)\mathbf{T}_{k-1}^{-1}\mathbf{a}(\theta_0) \quad (20a)$$

$$\xi_k \triangleq \mathbf{a}^H(\theta_k)\mathbf{T}_{k-1}^{-1}\mathbf{a}(\theta_k) \quad (20b)$$

$$\xi_c \triangleq \mathbf{a}^H(\theta_k)\mathbf{T}_{k-1}^{-1}\mathbf{a}(\theta_0) \quad (20c)$$

$$\tilde{\xi}_c \triangleq \mathbf{a}^H(\theta_0)\mathbf{T}_{k-1}^{-1}\mathbf{a}(\theta_k). \quad (20d)$$

Then, from Proposition 1, problem (18) can be expressed as

$$\underset{\gamma_k}{\text{maximize}} \quad |\xi_0/\tilde{\xi}_c + \gamma_k| \quad (21a)$$

$$\text{subject to} \quad [\Re(\gamma_k) \ \Im(\gamma_k)]^T \in \mathbb{C}_\gamma. \quad (21b)$$

Although the problem (21) is non-convex, it will be shown that it can be analytically solved as follows.

Proposition 2: Denote the intersections of the circle and the line connecting the origin $\mathbf{O} = [0, 0]^T$ and the center \mathbf{c}_γ in (15) as $F_a \triangleq [\Re(\gamma_{k,a}) \ \Im(\gamma_{k,a})]^T$ and $F_b \triangleq [\Re(\gamma_{k,b}) \ \Im(\gamma_{k,b})]^T$, respectively, and assume that $|\gamma_{k,a}| < |\gamma_{k,b}|$. If \mathbf{T}_{k-1} is Hermitian (note that the Hermitian property of \mathbf{T}_{k-1} has

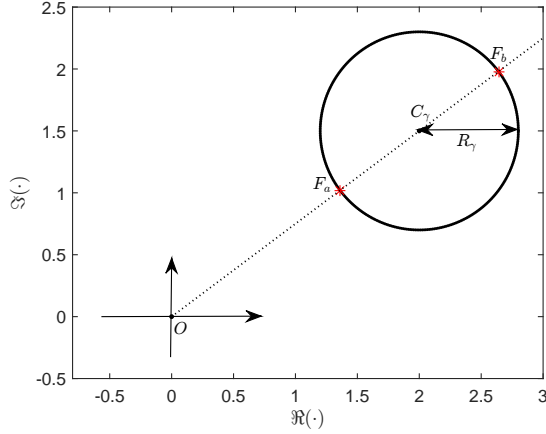


Fig. 1. Geometric distribution of γ_k .

not been guaranteed as we have mentioned earlier), then the optimal solution of (21) satisfies

$$\gamma_{k,\star} = \begin{cases} \gamma_{k,a}, & \text{if } \zeta > 0 \\ \gamma_{k,b}, & \text{otherwise} \end{cases} \quad (22)$$

where

$$\zeta \triangleq \text{sign}[\mathbf{c}_\gamma(1)] \cdot \text{sign}[\Re(d) - \mathbf{c}_\gamma(1)] \quad (23)$$

and

$$d \triangleq -\xi_0/\xi_c^*. \quad (24)$$

In addition, $\gamma_{k,a}$ and $\gamma_{k,b}$ in (22) are calculated as

$$\gamma_{k,a} = -\frac{(\|\mathbf{c}_\gamma\|_2 - R_\gamma)\chi\xi_c}{\|\mathbf{c}_\gamma\|_2\mathbf{H}_k(2,2)}, \quad \gamma_{k,b} = -\frac{(\|\mathbf{c}_\gamma\|_2 + R_\gamma)\chi\xi_c}{\|\mathbf{c}_\gamma\|_2\mathbf{H}_k(2,2)}$$

where $\chi = \xi_k - \rho_k\xi_0 \in \mathbb{R}$, \mathbf{c}_γ and R_γ are defined in Proposition 1.

Proof: See Appendix A. \blacksquare

To have a better understanding, the locations of $\gamma_{k,a}$ and $\gamma_{k,b}$ have been illustrated in Fig. 1. Obviously, once the optimal $\gamma_{k,\star}$ has been obtained, we can update the weight vector as

$$\mathbf{w}_k = \mathbf{w}_{k-1} + \gamma_{k,\star}\mathbf{v}_k. \quad (25)$$

This completes the update of weight vector of the k th step.

D. Update of the Inversion of VCM

Since the calculation of $\gamma_{k,\star}$ requires the inversion of VCM (i.e., \mathbf{T}_{k-1}^{-1}) which is assumed to be Hermitian in Proposition 2, in the sequel we shall discuss how to update \mathbf{T}_k^{-1} (in order to make the next step of response control feasible) and how to guarantee the Hermitian property. To address these two problems, we first assume that \mathbf{T}_{k-1} is Hermitian and the optimal $\gamma_{k,\star}$ has been obtained with the aid of Proposition 2. Then, from (9) we have

$$-\beta_{k,\star}/(1 + \beta_{k,\star}\xi_k) = \gamma_{k,\star}/\xi_c \quad (26)$$

Algorithm 1 OPARC Algorithm

- 1: give the initial weight vector $\mathbf{w}_0 = \mathbf{a}(\theta_0)$ and set $\mathbf{T}_0 = \mathbf{I}$, prescribe the direction θ_k and the corresponding desired level ρ_k , $k = 1, 2, \dots$
- 2: **for** $k = 1, 2, \dots$, **do**
- 3: calculate $\gamma_{k,\star}$ from (22) and obtain \mathbf{v}_k from (11)
- 4: update \mathbf{w}_k as $\mathbf{w}_k = \mathbf{w}_{k-1} + \gamma_{k,\star}\mathbf{v}_k$
- 5: update \mathbf{T}_k^{-1} as $\mathbf{T}_k^{-1} = \mathbf{T}_{k-1}^{-1} + \gamma_{k,\star}\mathbf{v}_k\mathbf{v}_k^H/\xi_c$
- 6: **end for**
- 7: output \mathbf{w}_k directly

where $\beta_{k,\star} = \Psi_k^{-1}(\gamma_{k,\star})$ denotes the INR corresponding to $\gamma_{k,\star}$ in the k th step. Obviously, the combination of (7) and (26) yields

$$\mathbf{T}_k^{-1} = \mathbf{T}_{k-1}^{-1} + \frac{\gamma_{k,\star}\mathbf{v}_k\mathbf{v}_k^H}{\xi_c}. \quad (27)$$

Therefore, \mathbf{T}_k^{-1} can be calculated out straightforwardly (without the calculation of \mathbf{T}_k and its inversion), once the optimal $\gamma_{k,\star}$ obtained.

To further explore the Hermitian property of \mathbf{T}_k , let us revisit Proposition 2 and get

$$\frac{\gamma_{k,\star}}{\xi_c} = -\frac{(\|\mathbf{c}_\gamma\|_2 \pm R_\gamma)\chi}{\|\mathbf{c}_\gamma\|_2\mathbf{H}_k(2,2)} \in \mathbb{R} \quad (28)$$

which is a real-valued number. Thus, it is known that \mathbf{T}_k is Hermitian as long as \mathbf{T}_{k-1} is Hermitian. Accordingly, it can be readily concluded that if we set $\mathbf{T}_0 = \mathbf{I}$, then \mathbf{T}_i is Hermitian for $i = 1, 2, \dots, k$.

Now, it is seen that the response levels can be successively adjusted by assigning virtual interferences. Therefore, we can utilize the above update procedures iteratively to fulfill the prescribed response control requirement. Finally, the proposed OPARC method is summarized in Algorithm 1.

III. SOME PROPERTIES OF OPARC

In the previous section, we have shown that the response level at a certain direction can be optimally and flexibly adjusted by assigning a virtual interference. Instead of determining β_k (i.e., the INR of the virtual interference assigned in the k th step), an alternative parameter γ_k , mapping of β_k , is chosen to facilitate the algorithm derivation. However, since INR has a physical meaning and is always a non-negative value in a real data case, it is worth examining the direct relationship between the response level and β_k . To do so, in this section we continue the analysis on the OPARC scheme, mainly focus on the selection of INR β_k rather than its mapping γ_k .

A. Geometrical Distribution of β_k

As shown in (9), γ_k is a mapping of β_k , and β_k can be expressed with respect to γ_k as

$$\beta_k = -\gamma_k/(\xi_c + \gamma_k\xi_k) = \Psi_k^{-1}(\gamma_k) \quad (29)$$

where $\Psi_k^{-1}(\cdot)$ is the inverse function of $\Psi_k(\cdot)$ in (9). Thus, β_k can be calculated once γ_k is available. For the trajectory

of β_k when the array response level ρ_k is satisfied at angle θ_k , let us recall Proposition 1 and express γ_k as

$$\gamma_k = \mathbf{c}_\gamma(1) + j\mathbf{c}_\gamma(2) + R_\gamma e^{j\varphi} \quad (30)$$

where \mathbf{c}_γ and R_γ are the center and the radius of the circle given in Proposition 1, φ can be any real-valued number. Substituting (30) into (29), one gets

$$\beta_k = (p_1 + p_2 e^{j\varphi}) / (q_1 + q_2 e^{j\varphi}) \quad (31)$$

where p_l and q_l ($l = 1, 2$) are complex numbers satisfying

$$p_1 = -\mathbf{c}_\gamma(1) - j\mathbf{c}_\gamma(2), \quad p_2 = -R_\gamma \quad (32a)$$

$$q_1 = \xi_c + (\mathbf{c}_\gamma(1) + j\mathbf{c}_\gamma(2)) \xi_k, \quad q_2 = R_\gamma \xi_k. \quad (32b)$$

With some calculation, it is not difficult to have the following proposition.

Proposition 3: The trajectory of $[\Re(\beta_k) \ \Im(\beta_k)]^T$ with β_k satisfying (31) is a circle \mathbb{C}_β with the center

$$\mathbf{c}_\beta = [\xi_0 / (|\xi_c|^2 - \xi_0 \xi_k), \ 0]^T \quad (33)$$

and the radius

$$R_\beta = |\xi_c| / [\sqrt{\rho_k} \cdot (|\xi_c|^2 - \xi_0 \xi_k)] \quad (34)$$

i.e.,

$$\beta_k = \mathbf{c}_\beta(1) + j\mathbf{c}_\beta(2) + R_\beta e^{j\phi} \quad (35)$$

where ϕ can be any real-valued number.

Similar to γ_k , all the β_k on the above circle can be used to precisely adjust the response level at θ_k to its desired level ρ_k . An interesting difference with γ_k is that the calculations of \mathbf{c}_β and R_β do not require the knowledge of \mathbf{w}_{k-1} . This implies that all β_k 's (including the optimal one later) can be obtained without knowing any weight vectors. On the contrary, the determination of γ_k relies on the availability of the previous weight vector \mathbf{w}_{k-1} .

In addition, Proposition 3 implies that the center of the trajectory of $[\Re(\beta_k) \ \Im(\beta_k)]^T$ is located on the real axis, and is independent of the desired level ρ_k .

B. Determination of the Optimal β_k

Among all the valid β_k for the control of the array response level ρ_k at θ_k , the optimal one is the one that maximizes the array gain. Therefore, the following constrained optimization problem can be formulated to select the optimal β_k :

$$\underset{\beta_k}{\text{maximize}} \quad G_k = |\mathbf{w}_k^H \mathbf{a}(\theta_0)|^2 / |\mathbf{w}_k^H \mathbf{T}_k \mathbf{w}_k| \quad (36a)$$

$$\text{subject to} \quad L(\theta_k, \theta_0) = \rho_k \quad (36b)$$

$$\mathbf{w}_k = \mathbf{w}_{k-1} + \Psi_k(\beta_k) \mathbf{T}_{k-1}^{-1} \mathbf{a}(\theta_k) \quad (36c)$$

where the parameter γ_k has been replaced in (36c) by $\Psi_k(\beta_k)$. Clearly, the above optimization problem (36) is equivalent to problem (18). Therefore, the optimal solution (denoted as $\beta_{k,\star}$) of (36) can be readily obtained by utilizing the mapping as

$$\beta_{k,\star} = \Psi_k^{-1}(\gamma_{k,\star}). \quad (37)$$

Combining the result of $\gamma_{k,\star}$ in (22) with some calculation, we can derive Proposition 4 below.

Algorithm 2 OPARC Algorithm (an Equivalent Variant)

- 1: give $\mathbf{a}(\theta_0)$ and set $\mathbf{T}_0 = \mathbf{I}$, specify the direction θ_k and the corresponding desired level ρ_k with $k = 1, 2, \dots$
 - 2: **for** $k = 1, 2, \dots$, **do**
 - 3: calculate $\beta_{k,\star}$ from (38)
 - 4: update \mathbf{T}_k as $\mathbf{T}_k = \mathbf{T}_{k-1} + \beta_{k,\star} \mathbf{a}(\theta_k) \mathbf{a}^H(\theta_k)$
 - 5: **end for**
 - 6: calculate $\mathbf{w}_k = \mathbf{T}_k^{-1} \mathbf{a}(\theta_0)$
-

Proposition 4: The optimal solution of (36) is given by

$$\beta_{k,\star} = \begin{cases} \beta_{k,r}, & \text{if } -1/\xi_k > \xi_0 / (|\xi_c|^2 - \xi_0 \xi_k) \\ \beta_{k,l}, & \text{otherwise} \end{cases} \quad (38)$$

where $\beta_{k,r}$ and $\beta_{k,l}$ are the intersections of circle \mathbb{C}_β and the real axis $\Im(\cdot) = 0$:

$$\beta_{k,r} = R_\beta + \xi_0 / (|\xi_c|^2 - \xi_0 \xi_k) \quad (39)$$

$$\beta_{k,l} = -R_\beta + \xi_0 / (|\xi_c|^2 - \xi_0 \xi_k). \quad (40)$$

It is not hard to see from (38) that the optimal $\beta_{k,\star}$ is a real-valued number, while the valid β_k in Proposition 3 for the array response control may be complex valued. However, as mentioned earlier, the physical meaning of β_k is the INR as it is used in (5) and it cannot be negative. From (38)-(40), the solved optimal $\beta_{k,\star}$ may be negative, which might be because there is no assumption of the used VCM \mathbf{T}_{k-1} being non-negative definite. This will be studied together with the update of the VCM below. On the other hand, if \mathbf{T}_{k-1} is Hermitian, then $\mathbf{T}_k = \mathbf{T}_{k-1} + \beta_{k,\star} \mathbf{a}(\theta_k) \mathbf{a}^H(\theta_k)$ is also Hermitian, since $\beta_{k,\star}$ is real. This is consistent with the inference obtained in the paragraph below Eqn. (28). Finally, it is obvious that the optimal β_k in (38) does not depend on the knowledge of the weight vectors in the previous steps.

Once the optimal β_k has been obtained, we can express the VCM at the current stage as

$$\mathbf{T}_k = \mathbf{T}_{k-1} + \beta_{k,\star} \mathbf{a}(\theta_k) \mathbf{a}^H(\theta_k) = \mathbf{I} + \mathbf{A}_k \mathbf{\Sigma}_k \mathbf{A}_k^H \quad (41)$$

where $\mathbf{A}_k \triangleq [\mathbf{a}(\theta_1), \dots, \mathbf{a}(\theta_k)]$ and $\mathbf{\Sigma}_k$ is a diagonal matrix containing all β 's of virtual interferences, i.e.,

$$\mathbf{\Sigma}_k = \text{Diag}([\beta_{1,\star}, \beta_{2,\star}, \dots, \beta_{k,\star}]). \quad (42)$$

Accordingly, we have $\mathbf{w}_k = \mathbf{T}_k^{-1} \mathbf{a}(\theta_0)$. To make it clear, the variant of the OPARC method is summarized in Algorithm 2. Note that the calculation of intermediate weight vectors is avoided, due to the fact that neither the calculation of $\beta_{k,\star}$ nor \mathbf{T}_k relies on weight vectors. Therefore, the procedure of array response control is simplified.

Before proceeding, it is interesting to provide a deep insight and a geometrical perspective on the relationship between γ_k and β_k . It is not hard to see that the condition $-1/\xi_k > \xi_0 / (|\xi_c|^2 - \xi_0 \xi_k)$ in (38) is equivalent to the condition $\zeta > 0$ in (22), if and only if $\rho_k \xi_0 < \xi_k$. It implies that the conditions for selecting $\beta_{k,\star}$ between $\beta_{k,l}$ and $\beta_{k,r}$ and selecting $\gamma_{k,\star}$ between $\gamma_{k,a}$ and $\gamma_{k,b}$ may be different and are the same under a certain condition, i.e., $\rho_k \xi_0 < \xi_k$. Thus, we have

$$\begin{cases} \gamma_{k,a} = \Psi_k(\beta_{k,r}), \gamma_{k,b} = \Psi_k(\beta_{k,l}), & \text{if } \rho_k \xi_0 < \xi_k \\ \gamma_{k,a} = \Psi_k(\beta_{k,l}), \gamma_{k,b} = \Psi_k(\beta_{k,r}), & \text{otherwise.} \end{cases} \quad (43)$$

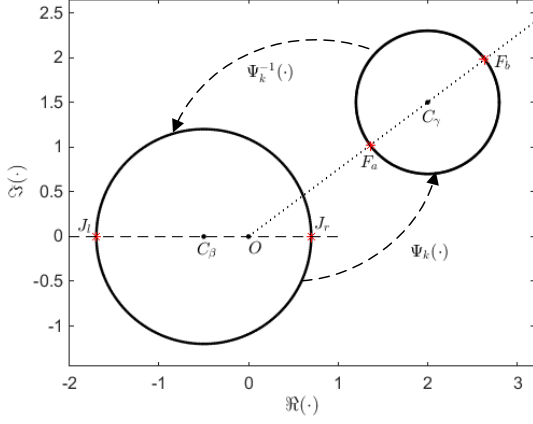


Fig. 2. Illustration of the mapping $\Psi_k(\cdot)$.

To have an intuitive perspective on $\Psi_k(\cdot)$, a geometrical illustration is given in Fig. 2, where J_r , J_l , F_a and F_b stand for the points $[\Re(\beta_{k,r}) \ \Im(\beta_{k,r})]^T$, $[\Re(\beta_{k,l}) \ \Im(\beta_{k,l})]^T$, $[\Re(\gamma_{k,a}) \ \Im(\gamma_{k,a})]^T$ and $[\Re(\gamma_{k,b}) \ \Im(\gamma_{k,b})]^T$, respectively.

C. Positive Definite Virtual Covariance Matrices

Firstly, the following conclusion, which simplifies the selection of $\beta_{k,\star}$, can be obtained.

Proposition 5: If $\mathbf{T}_{k-1} \in \mathbb{S}_{++}^N$, we have

$$\beta_{k,\star} = \beta_{k,r} = (|\xi_c| - \sqrt{\rho_k} \xi_0) / [\sqrt{\rho_k} (\xi_0 \xi_k - |\xi_c|^2)]. \quad (44)$$

Furthermore, if $\mathbf{T}_{k-1} \in \mathbb{S}_{++}^N$, then $\mathbf{T}_k \in \mathbb{S}_{++}^N$ if and only if $\rho_k < \xi_k^2 / |\xi_c|^2$.

Proof: See Appendix B. ■

Similar to the argument in the paragraph below Eqn. (17), $\xi_k^2 / |\xi_c|^2$ is in general greater than 1 and it is assumed $\rho_k \leq 1$. Thus, we have $\rho_k < \xi_k^2 / |\xi_c|^2$. As a consequence, in each step of weight vector update, we have $\mathbf{T}_k \in \mathbb{S}_{++}^N$ and $\beta_{k,\star} = \beta_{k,r}$, as long as $\mathbf{T}_{k-1} \in \mathbb{S}_{++}^N$. Since in our algorithm $\mathbf{T}_0 = \mathbf{I}$ is taken as the initial VCM, we have $\mathbf{T}_k \in \mathbb{S}_{++}^N$ and $\beta_{k,\star} = \beta_{k,r}$.

Proposition 6: If $\mathbf{T}_{k-1} \in \mathbb{S}_{++}^N$, then

$$\beta_{k,\star} \geq 0 \Leftrightarrow |\xi_c| \geq \sqrt{\rho_k} \xi_0 \quad (45a)$$

$$\beta_{k,\star} < 0 \Leftrightarrow |\xi_c| < \sqrt{\rho_k} \xi_0. \quad (45b)$$

Proof: From (68) in the proof of Proposition 5 in Appendix B, we have $\xi_0 \xi_k - |\xi_c|^2 > 0$ provided that $\mathbf{T}_{k-1} \in \mathbb{S}_{++}^N$. Then, from (44), the proof of (45) is completed. ■

Substituting the definitions of ξ_c and ξ_0 into (45) and using $\mathbf{w}_{k-1} = \mathbf{T}_{k-1}^{-1} \mathbf{a}(\theta_0)$, we have

$$\beta_{k,\star} \geq 0 \Leftrightarrow \rho_k \leq \frac{|\mathbf{w}_{k-1}^H \mathbf{a}(\theta_k)|^2}{|\mathbf{w}_{k-1}^H \mathbf{a}(\theta_0)|^2} \quad (46a)$$

$$\beta_{k,\star} < 0 \Leftrightarrow \rho_k > \frac{|\mathbf{w}_{k-1}^H \mathbf{a}(\theta_k)|^2}{|\mathbf{w}_{k-1}^H \mathbf{a}(\theta_0)|^2}. \quad (46b)$$

Notice that $|\mathbf{w}_{k-1}^H \mathbf{a}(\theta_k)|^2 / |\mathbf{w}_{k-1}^H \mathbf{a}(\theta_0)|^2$ above represents the normalized response at θ_k , of the previous weight vector \mathbf{w}_{k-1} . Clearly, (46) shows that the resultant $\beta_{k,\star}$ is non-negative if the desired level ρ_k is lower than the response level at θ_k of the previous weight vector \mathbf{w}_{k-1} . Otherwise, a negative $\beta_{k,\star}$ is obtained if it is required to elevate the previous

response level of θ_k . We can see that the negative $\beta_{k,\star}$ is still meaningful in our discussion of array response control using virtual interferences, although it cannot occur in a real data covariance matrix with real interferences.

In addition to the above two propositions, the following result can be obtained.

Proposition 7: If $\mathbf{T}_{k-1} \in \mathbb{S}_{++}^N$, then problem (36) has the same optimal solution as that of the following one

$$\underset{\beta_k}{\text{maximize}} \quad \frac{|\mathbf{w}_k^H \mathbf{a}(\theta_0)|^2}{\mathbf{w}_k^H \mathbf{T}_{k-1} \mathbf{w}_k} \quad (47a)$$

$$\text{subject to} \quad L(\theta_k, \theta_0) = \rho_k \quad (47b)$$

$$\mathbf{w}_k = \mathbf{w}_{k-1} + \Psi_k(\beta_k) \mathbf{v}_k. \quad (47c)$$

Proof: See Appendix C. ■

Interestingly, from Proposition 7, it is known that under the same constraints (i.e., (36b) and (36c)), the optimal β_k to (36) also maximizes the previous array gain, in which only \mathbf{T}_{k-1} (but not \mathbf{T}_k) is taken into consideration.

For instance, consider the case when \mathbf{T}_{k-1} is a real normalized noise-plus-interference covariance matrix (i.e., \mathbf{T}_{k-1} is calculated from real data that contains both noise and interference), and one applies the OPARC scheme to realize a specific array response control task in (47b) by assigning a virtual interference at θ_k . Then, it is seen from Proposition 7 that the optimal $\beta_{k,\star}$ of problem (36) also maximizes the real output SINR (not taking the virtual interference into consideration) of beamformer. This property will be further exploited in the companion paper [19] to design an adaptive beamformer with specific constraint.

IV. COMPARISON WITH A²RC

In the above sections, the optimal values of γ_k and β_k of the virtual interference assigned in the k th step are specified. Meanwhile, useful conclusions are obtained and two versions of OPARC are described. In this section, comparisons will be carried out to elaborate the differences between the recent A²RC algorithm [15] and the above OPARC algorithm from two perspectives.

A. Comparison on the Formula Updating

In the A²RC method, the weight vector is updated as

$$\mathbf{w}_k = \mathbf{w}_{k-1} + \mu_k \mathbf{a}(\theta_k) \quad (48)$$

where μ_k is the hyperparameter to be optimized. To minimize the deviation between the resultant responses of adjacent two steps, and meanwhile, avoid the computationally inefficient global search, μ_k is empirically selected in [15] as $\mu_{k,a}$, which is the solution to the following problem:

$$\underset{\mu_k}{\text{minimize}} \quad |\mu_k| \quad (49a)$$

$$\text{subject to} \quad [\Re(\mu_k) \ \Im(\mu_k)]^T \in \mathbb{C}_\mu \quad (49b)$$

where \mathbb{C}_μ is the following circle:

$$\mathbb{C}_\mu = \left\{ [\Re(\mu_k) \ \Im(\mu_k)]^T \mid \left\| [\Re(\mu_k) \ \Im(\mu_k)]^T - \mathbf{c}_\mu \right\|_2 = R_\mu \right\}$$

with the center

$$\mathbf{c}_\mu = \frac{1}{\mathbf{Q}_k(2, 2)} \begin{bmatrix} -\Re[\mathbf{Q}_k(1, 2)] \\ \Im[\mathbf{Q}_k(1, 2)] \end{bmatrix} \quad (50)$$

and the radius

$$R_\mu = \sqrt{-\det(\mathbf{Q}_k)/|\mathbf{Q}_k(2, 2)|} \quad (51)$$

where the matrix \mathbf{Q}_k satisfies

$$\mathbf{Q}_k = [\mathbf{w}_{k-1} \ \mathbf{a}(\theta_k)]^H (\mathbf{a}(\theta_k) \mathbf{a}^H(\theta_k) - \rho_k \mathbf{a}(\theta_0) \mathbf{a}^H(\theta_0)) [\mathbf{w}_{k-1} \ \mathbf{a}(\theta_k)].$$

Note that such an empirical selection may not perform well under all circumstances. As a matter of fact, this scheme may even lead to severe pattern distortion, as we will show later in simulations in Section V.

In the OPARC algorithm, the weight vector is updated via (18c). It is seen that, different from the A²RC algorithm, a scaling of $\mathbf{T}_{k-1}^{-1} \mathbf{a}(\theta_k)$ is added to \mathbf{w}_{k-1} , and $\gamma_k \mathbf{T}_{k-1}^{-1} \mathbf{a}(\theta_k)$ makes the resultant \mathbf{w}_k be an optimal weight vector.

Additionally, in the proposed OPARC algorithm, we optimize the parameter γ_k by maximizing the array gain when the preassigned response level is satisfied.

To have a similar weight form with A²RC, it is shown in Appendix D that we can reformulate (18c) as

$$\begin{aligned} \mathbf{w}_k &= \mathbf{w}_{k-1} + \gamma_k \mathbf{A}(\theta_k, \dots, \theta_1) \mathbf{d}_k \\ &= \mathbf{w}_{k-1} + \gamma_k \mathbf{a}(\theta_k) + \gamma_k \mathbf{A}(\theta_{k-1}, \dots, \theta_1) \bar{\mathbf{d}}_k \end{aligned} \quad (52)$$

where $\mathbf{A}(\theta_k, \dots, \theta_1) \triangleq [\mathbf{a}(\theta_k), \dots, \mathbf{a}(\theta_1)]$, with θ_i ($1 \leq i \leq k-1$) denoting the angles of interferences that assigned previously, \mathbf{d}_k is a $k \times 1$ vector with its first element 1, $\bar{\mathbf{d}}_k$ is a $(k-1) \times 1$ vector obtained by removing the first element from \mathbf{d}_k . From (52), it is observed that the added component to the previous weight vector \mathbf{w}_{k-1} in \mathbf{w}_k is a linear combination of the steering vectors of all interferences (including both the current $\mathbf{a}(\theta_k)$ and the previous $\mathbf{a}(\theta_1), \dots, \mathbf{a}(\theta_{k-1})$). On the contrary, in the A²RC algorithm, the added component is a scaling of the steering vector of the single interference to be assigned (i.e., $\mathbf{a}(\theta_k)$). Furthermore, we can obtain the following corollary of Proposition 2, which describes a similarity between A²RC and OPARC.

Corollary 1: In the first step of weight update (i.e., $\mathbf{w}_0 = \mathbf{a}(\theta_0)$, $\mathbf{T}_0 = \mathbf{I}$), if $\rho_1 \leq \|\mathbf{a}(\theta_1)\|_2^2 / \|\mathbf{a}(\theta_0)\|_2^2$, then $\mu_{1,\star} = \gamma_{1,\star}$, otherwise, $\mu_{1,\star} = \gamma_{1,\times}$, where $\gamma_{1,\times} = \{\gamma_{1,a}, \gamma_{1,b}\} \setminus \gamma_{1,\star}$.

Proof: See Appendix E. ■

From Corollary 1, it is known that in the first step of the weight vector update, A²RC will lead to the same result as OPARC, provided that $\rho_1 \leq \|\mathbf{a}(\theta_1)\|_2^2 / \|\mathbf{a}(\theta_0)\|_2^2$. Otherwise, the inferior parameter $\gamma_{1,\times}$ (in the sense of array gain) will be adopted by A²RC.

B. Comparison on INRs of Virtual Interferences

We next compare the INRs of virtual interferences to show an essential difference between A²RC and OPARC. To begin with, we express the weight vector of A²RC in the k th step as

$$\begin{aligned} \mathbf{w}_k &= \mathbf{a}(\theta_0) + \mu_1 \mathbf{a}(\theta_1) + \dots + \mu_k \mathbf{a}(\theta_k) \\ &= \mathbf{a}(\theta_0) + \mathbf{A}_k \mathbf{b}_k \end{aligned} \quad (53)$$

where $\mathbf{b}_k \triangleq [\mu_1, \mu_2, \dots, \mu_k]^T$. Note from the above that the update of the weight vector \mathbf{w}_k in A²RC does not depend on any VCM and no VCM update is needed. However, in order to compare the INRs, we need to associate it to a VCM that may be implicit/virtual. To do so, we rewrite the weight vector as

$$\begin{aligned} \mathbf{w}_k &= \check{\mathbf{T}}_k^{-1} \mathbf{a}(\theta_0) \\ &= \mathbf{a}(\theta_0) - \mathbf{A}_k \left(\mathbf{I} + \check{\mathbf{\Sigma}}_k \mathbf{A}_k^H \mathbf{A}_k \right)^{-1} \check{\mathbf{\Sigma}}_k \mathbf{A}_k^H \mathbf{a}(\theta_0) \end{aligned} \quad (54)$$

where $\check{\mathbf{T}}_k = \mathbf{I} + \mathbf{A}_k \check{\mathbf{\Sigma}}_k \mathbf{A}_k^H$ denotes a VCM, $\check{\mathbf{\Sigma}}_k = \text{Diag}([\check{\beta}_{k,1}, \check{\beta}_{k,2}, \dots, \check{\beta}_{k,k}])$ specifies the INR of the interference at θ_i ($i = 1, \dots, k$) when completing the current k th step of the weight vector update.

Note that no interference was assigned at the current θ_k in the previous $k-1$ steps of the response control. It is shown from Appendix F that in the k th step of the weight update of the A²RC algorithm, the INR of the virtual interference assigned at θ_k is

$$\check{\beta}_{k,k} = -\frac{\mu_k}{\mathbf{a}^H(\theta_k) \check{\mathbf{w}}_{k-1} + \mu_k \|\mathbf{a}(\theta_k)\|_2^2}. \quad (55)$$

In addition, $k-1$ new interferences are additively assigned at directions $\theta_1, \dots, \theta_{k-1}$ of A²RC to the previous $(k-1)$ th step. Denote the INRs of these new interferences assigned at θ_i in the k th step of the weight update as $\check{\Delta}_{k,i}$ ($1 \leq i \leq k-1$). Clearly they satisfy

$$\check{\Delta}_{k,i} = \check{\beta}_{k,i} - \check{\beta}_{k-1,i}. \quad (56)$$

It can be further derived (see Appendix F) that

$$\check{\Delta}_{k,i} = \frac{\mu_k \mathbf{a}^H(\theta_i) \mathbf{a}(\theta_k) \check{\beta}_{k-1,i}^2}{\mu_i - \mu_k \mathbf{a}^H(\theta_i) \mathbf{a}(\theta_k) \check{\beta}_{k-1,i}}. \quad (57)$$

Generally speaking, in the k th step of A²RC, the INRs of the newly-assigned interferences (including both $\check{\beta}_{k,k}$ and $\check{\Delta}_{k,i}$ ($1 \leq i \leq k-1$)) are complex-valued numbers. This is a difference between A²RC and OPARC. Moreover, the above analysis shows that there are $k-1$ additional interferences assigned to the previously controlled angles (i.e., $\theta_1, \dots, \theta_{k-1}$) in the k th step of A²RC, while in OPARC only a single interference is assigned (at θ_k). Since our aim is to control the array response level at θ_k , the newly-assigned virtual interferences at $\theta_1, \dots, \theta_{k-1}$ actually bring undesirable array response variations at these adjusted angles. According to the above notations, the VCM of A²RC satisfies implicitly:

$$\check{\mathbf{T}}_k = \check{\mathbf{T}}_{k-1} + \mathbf{A}_k \text{Diag}([\check{\Delta}_{k,1}, \dots, \check{\Delta}_{k,k-1}, \check{\beta}_{k,k}]) \mathbf{A}_k^H \quad (58)$$

which is different from that of OPARC in (41).

To summarize, the main differences between the proposed OPARC algorithm and the existing A²RC algorithm include:

- Different formulas of the weight update are employed in OPARC and A²RC.
- The resultant weight of OPARC can be guaranteed to be an optimal beamformer, while A²RC method does not.
- The array gain is introduced to the parameter optimization of OPARC, while A²RC is not.

- The update of VCM is necessary for OPARC, while A²RC is free of this procedure although its VCM is implicitly updated by (58).
- Two different strategies of virtual interference assigning are adopted in these two approaches. The INRs of OPARC are always real, but they may not be in A²RC.

V. SIMULATION RESULTS

We next present some simulations to verify the effectiveness of our proposed OPARC. To validate the superiority of OPARC, we also test another precise array response control (PARC) scheme, in which we adopt the following non-optimal parameter intentionally:

$$\gamma_k = \gamma_{k,\times} \triangleq \{\gamma_{k,a}, \gamma_{k,b}\} \setminus \gamma_{k,\star} \quad (59)$$

and use the same remaining procedure as OPARC. Denote $\beta_{k,\times} = \Psi_k^{-1}(\gamma_{k,\times})$. Note that $\gamma_{1,\times}$ is the same as that in Corollary 1. Clearly, PARC can precisely control array response level as well, while its parameter γ_k is not optimally selected as in OPARC. Besides OPARC and PARC, the A²RC algorithm in [15] is also compared. We set $\omega = 6\pi \times 10^8$ rad/s, which corresponds to a wavelength $\lambda = 2\pi c/\omega = 1$ m with the light speed c . Consider a 11-element nonuniform spaced linear array with nonisotropic elements. Both the element locations x_n and the element patterns $g_n(\theta)$ are listed in Table I, from which the $\tau_n(\theta)$ in (2) can be specified as $\tau_n(\theta) = x_n \sin(\theta)/c$. Additionally, we take the quiescent weight vector $\mathbf{a}(\theta_0)$ as the initial weight and fix the beam axis at $\theta_0 = 20^\circ$ for all experiments conducted. For convenience, we carry out two steps of the array response control algorithms and denote the two adjusted angles as θ_1 and θ_2 , respectively.

To measure the performances of different methods, we introduce two cost functions. The first one is defined as

$$D \triangleq |L_2(\theta_1, \theta_0) - L_1(\theta_1, \theta_0)| \quad (60)$$

where $L_k(\theta, \theta_0)$ represents the resultant response after finishing the k -th step of weight update. It is seen that D measures the response level difference between two consecutive response controls at θ_1 . The second cost function is defined as

$$J \triangleq \sqrt{\frac{1}{I} \sum_{i=1}^I |L_2(\vartheta_i, \theta_0) - L_1(\vartheta_i, \theta_0)|^2} \quad (61)$$

where ϑ_i stands for the i th sampling point in the angle sector, I denotes the number of sampling points. J measures the deviation between two response patterns L_2 and L_1 . We will uniformly sample the region $[-90^\circ, 90^\circ]$ every 0.2° and hence obtain $I = 901$ discrete points. Besides D and J above, we also test the obtained array gains of different methods, and consider pattern variation and pattern distortion for performance comparison.

A. Pattern Variation

In the first example, we test the performances of different approaches for sidelobe response control. More specifically, the normalized responses at $\theta_1 = -45^\circ$ and $\theta_2 = -5^\circ$ are

TABLE I
ELEMENT LOCATIONS AND ELEMENT PATTERNS OF THE NONUNIFORM LINEAR ARRAY

n	x_n	$g_n(\theta)$	n	x_n	$g_n(\theta)$
1	0.00	$1.00\cos(1.00\theta)$	7	3.05	$1.02\cos(1.00\theta)$
2	0.45	$0.98\cos(0.85\theta)$	8	3.65	$1.08\cos(0.90\theta)$
3	1.00	$1.05\cos(0.98\theta)$	9	4.03	$0.96\cos(0.75\theta)$
4	1.55	$1.10\cos(0.70\theta)$	10	4.60	$1.09\cos(0.92\theta)$
5	2.10	$0.90\cos(0.85\theta)$	11	5.00	$1.02\cos(0.80\theta)$
6	2.60	$0.93\cos(0.69\theta)$			

expected to be successively adjusted to $\rho_1 = -40$ dB and $\rho_2 = -30$ dB.

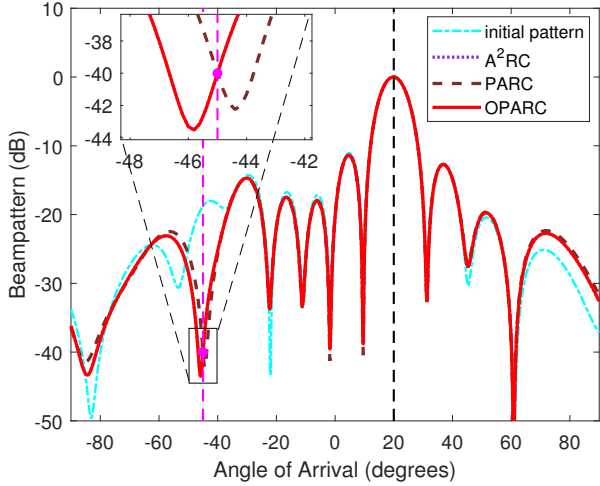
In the first step of response control, we can figure out that $\mathbf{c}_\gamma = [-0.1704, -0.0315]^T$, $d = -8.5231 - j1.5766$, $\gamma_{1,a} = -0.1559 - j0.0288$ and $\gamma_{1,b} = -0.1849 - j0.0342$. On this basis, we obtain that $\zeta = 1 > 0$ and hence choose $\gamma_{1,\star} = \gamma_{1,a}$ for OPARC and select $\gamma_{1,\times} = \gamma_{1,b}$ for PARC, according to (22) and (59), respectively. Additionally, it can be figured out that $\mathbf{c}_\beta = [-0.1488, 0]^T$ and $R_\beta = 1.7171$. We adopt $\beta_{1,\star} = \beta_{1,r} = 1.5683$ for OPARC and take $\beta_{1,\times} = \beta_{1,l} = -1.8659$ for PARC.

For A²RC, it is found that $\mu_1 = \gamma_{1,\star} = -0.1559 - j0.0288$, which coincides with the result of Corollary 1. As predicted, one also obtains that $\check{\beta}_{1,1} = \beta_{1,\star} = 1.5683$. Fig. 3(a) illustrates the resultant response patterns of different schemes. As we can see, all these three approaches are capable of precisely controlling the array response levels as expected. Notice also that the result of A²RC is exactly the same as that of OPARC.

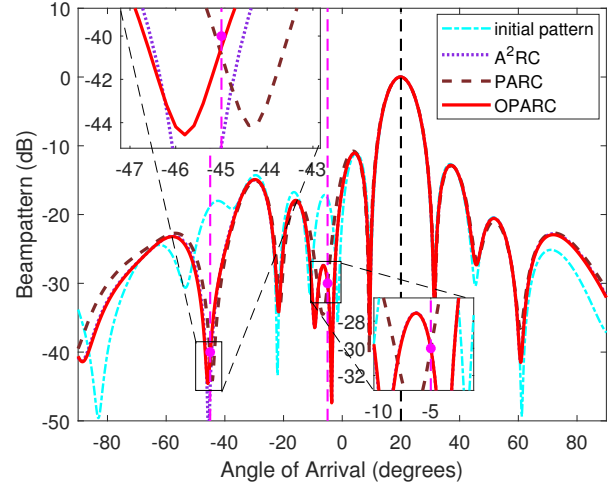
In the second step, with the same manner we found out that $\gamma_{2,\star} = -0.0685 - j0.0399$, $\beta_{2,\star} = 0.2504$, $\gamma_{2,\times} = -0.1148 - j0.0695$, $\beta_{2,\times} = -0.4277$ and $\mu_2 = -0.0674 - j0.0393$. Fig. 3(b) depicts the results of different methods. It is seen that all methods can adjust $L(\theta_2, \theta_0)$ to ρ_2 . For the proposed OPARC scheme, it can be checked that $\beta_{k,r}$ is the ultimate selection of $\beta_{k,\star}$ ($k = 1, 2$). In fact, this is consistent with the conclusion of Proposition 5. One can see that both $\beta_{1,\star}$ and $\beta_{2,\star}$ are positive in this case. This coincides with the theoretical prediction of Proposition 6, since it is required to lower the response levels in either step.

To further examine the performance, we evaluate D and J as defined earlier and list their measurements in Table II. It is observed that the proposed OPARC scheme minimizes both D and J among the three methods. From Table II and Fig. 3(b), it is found that A²RC causes serious perturbation (about 5 dB) at the previous point θ_1 . In fact, besides the virtual interference assigned at θ_2 , another one is also assigned at the previously adjusted direction (i.e., θ_1), for the existing A²RC algorithm. We can calculate that $\check{\beta}_{2,2} = 0.2465 + j0.0001$ and $\check{\Delta}_{2,1} = -0.4120 + j2.5879$ (INR of the additional interference assigned at θ_1 in the second step of response control). Notice that both $\check{\beta}_{2,2}$ and $\check{\Delta}_{2,1}$ are complex numbers, which is different from that of OPARC. Finally, we have listed the obtained array gains of these approaches at both steps in Table II. Clearly, it is seen that OPARC outperforms the other two methods.

Since both D and J depend on the desired level at θ_2 (i.e.,



(a) Comparison of synthesized patterns at the 1st step



(b) Comparison of synthesized patterns at the 2nd step

Fig. 3. Resultant pattern comparison (the first example).

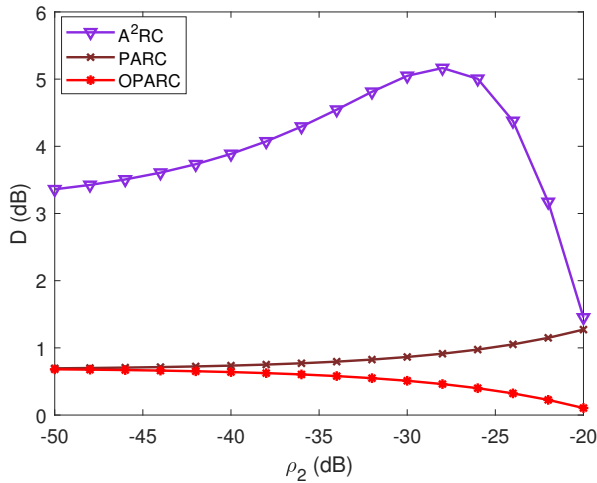
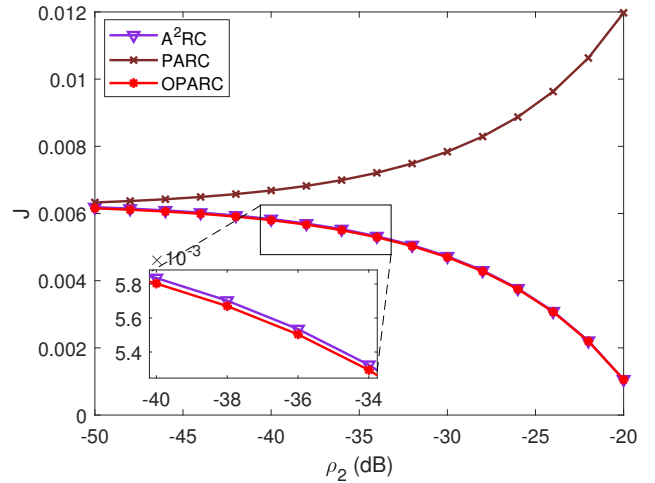
(a) Curves of D versus ρ_2 (b) Curves of J versus ρ_2

Fig. 4. Pattern variation comparison (the first example).

TABLE II
OBTAINED PARAMETER COMPARISON (THE FIRST EXAMPLE)

	A ² RC	PARC	OPARC
D (dB)	5.05	0.86	0.51
J	$4.72e^{-3}$	$7.84e^{-3}$	$4.69e^{-3}$
G_1 (dB)	10.0482	10.0331	10.0482
G_2 (dB)	10.0026	9.9653	10.0074

ρ_2), we vary ρ_2 from -50 dB to -20 dB and recalculate D and J with the other settings unchanged. Fig. 4(a) and Fig. 4(b) plot the curves of D versus ρ_2 and J versus ρ_2 , respectively. It can be clearly observed that the proposed OPARC algorithm performs the best on both D and J . The existing A²RC performs well on J , however, it causes a large deviation to the response level at θ_1 as displayed in Fig. 4(a).

B. Pattern Distortion

In this part, we shall further show the advantages of the OPARC. For convenience, we set θ_1 and its desired level ρ_1 the same as the first example, and then conduct the second step of the response control by taking $\theta_2 = 23^\circ$ and $\rho_2 = 0$ dB. Notice that θ_2 is in the mainlobe region in this case, and it is required to elevate the response level there.

Clearly, the obtained parameters of the second step are renewed for all methods tested, while the results of the first step keep unaltered compared to the previous example. Here, it can be obtained with the A²RC algorithm that $\mu_2 = -0.5931 + j0.8040$, $\beta_{2,2} = -0.3923 - j0.4011$ and $\Delta_{2,1} = -1.8001 + j0.0334$. For the PARC algorithm, we obtain $\gamma_{2,x} = -0.7108 + j0.7171$ and $\beta_{2,x} = -0.8522$. While for OPARC, its parameter satisfies $\gamma_{2,*} = \gamma_{2,b} = 0.8352 - j0.8438$ and $\beta_{2,*} = \beta_{2,r} = -0.0577$. It is worth noting that we have selected γ_b , which is different from that at Step 1 (where γ_a is selected), to obtain the final $\gamma_{2,*}$. In

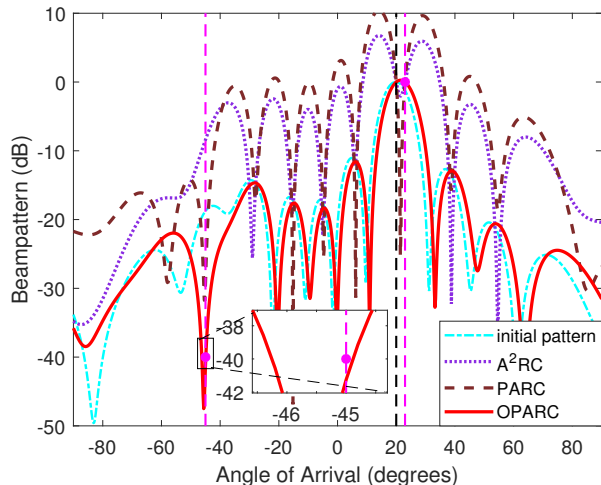


Fig. 5. Comparison of synthesized patterns at the 2nd step of the 2nd example.

TABLE III
OBTAINED PARAMETER COMPARISON (THE SECOND EXAMPLE)

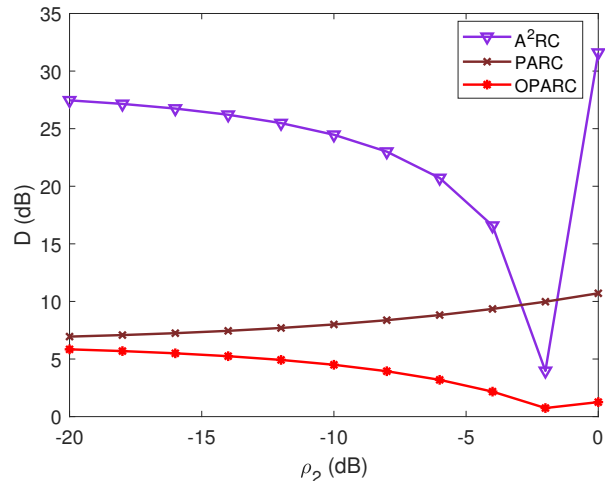
	A ² RC	PARC	OPARC
D (dB)	31.6001	10.7083	1.2595
J	1.0685	2.5149	0.0624
G_2 (dB)	2.5060	0.7366	13.1370

fact, this flexible mechanism of parameter determination in OPARC enables us to avoid certain pattern distortion, which is inevitable in A²RC or PARC. To see this clearer, we have depicted the synthesized patterns in Fig. 5. It can be found that all the response levels at θ_2 still meet the requirement as before. However, it shows clearly that the patterns of A²RC and PARC are severely distorted. The obtained mainlobes are split and the resultant sidelobe levels are raised for both A²RC and PARC. For the proposed OPARC, none of the above undesirable phenomena happens and a well-shaped pattern has been obtained. By the way, notice that $\beta_{2,*}$ is negative in this scenario. This is consistent with the conclusion of Proposition 6, since the response level needs to be lifted in this second step of response control.

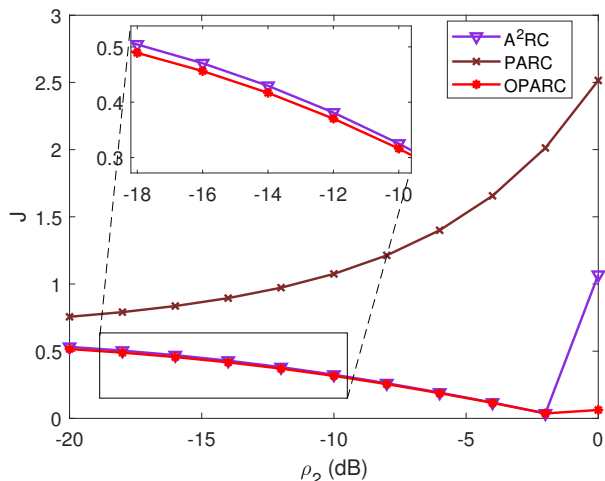
The details of D , J and the obtained array gains have been specified in Table III, from which the merits of the proposed OPARC algorithm are clearly observed. Note that the array gain G_1 is not listed in Table III since it has been reported in Table II. Again, to further examine the performance, we vary ρ_2 from -20 dB to 0 dB, and depict the curve of D versus ρ_2 in Fig. 6(a) and curve of J versus ρ_2 in Fig. 6(b), respectively. As illustrated in these two figures, A²RC causes a great perturbation on θ_1 (i.e., high value of D) and PARC performs poor on the average deviation J . On the other hand, OPARC performs the best when measuring either D or J .

VI. CONCLUSIONS

In this paper, a novel algorithm of optimal and precise array response control (OPARC) has been proposed. This algorithm originates from the adaptive array theory and the change rule of



(a) Curves of D versus ρ_2



(b) Curves of J versus ρ_2

Fig. 6. Pattern variation comparison (the second example).

the optimal weight vector, when adding interferences one by one, has been found. Then, the parameter selection mechanism has been carried out to maximize the array gain with the constraint that the response level at one direction is precisely adjusted. Some properties of OPARC have been presented and OPARC is compared in details with A²RC. Finally, simulation results have been shown to illustrate the effectiveness of the proposed OPARC method. Based on the fundamentals developed in this paper, a further extension of OPARC to multi-point array response control and its applications to, for example, pattern synthesis, multi-constraint adaptive beamforming and quiescent pattern control will be considered in [19].

APPENDIX A PROOF OF PROPOSITION 2

Since \mathbf{T}_{k-1} is assumed to be Hermitian, both ξ_0 and ξ_k are real-valued and one also gets $\hat{\xi}_c = \xi_c^*$. According to (14), we have

$$\mathbf{H}_k(1, 2) = \mathbf{w}_{k-1}^H [\mathbf{a}(\theta_k) \mathbf{a}^H(\theta_k) - \rho_k \mathbf{a}(\theta_0) \mathbf{a}^H(\theta_0)] \mathbf{v}_k = \chi \xi_c^*$$

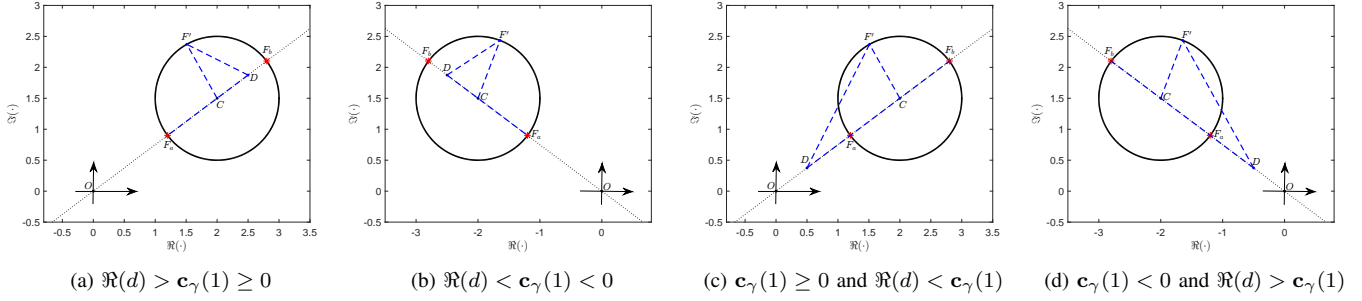


Fig. 7. Geometrical illustration of different cases when maximizing array gain.

where $\chi = \xi_k - \rho_k \xi_0 \in \mathbb{R}$. From (15), we have

$$\mathbf{c}_\gamma(1) + j\mathbf{c}_\gamma(2) = -\chi \xi_c / \mathbf{H}_k(2, 2). \quad (62)$$

Thus,

$$\gamma_{k,a} = -\frac{(\|\mathbf{c}_\gamma\|_2 - R_\gamma) \chi \xi_c}{\|\mathbf{c}_\gamma\|_2 \mathbf{H}_k(2, 2)}, \quad \gamma_{k,b} = -\frac{(\|\mathbf{c}_\gamma\|_2 + R_\gamma) \chi \xi_c}{\|\mathbf{c}_\gamma\|_2 \mathbf{H}_k(2, 2)}.$$

From (62) and both χ and $\mathbf{H}_k(2, 2)$ are real, we have

$$\mathbf{c}_\gamma(2) / \mathbf{c}_\gamma(1) = \Im(\xi_c) / \Re(\xi_c). \quad (63)$$

For the array gain G_k in (19) we have

$$\begin{aligned} G_k &= |\xi_c^*| \cdot |\xi_0 / \xi_c^* + \gamma_k| = |\xi_c^*| \cdot |\gamma_k - d| \\ &= |\xi_c^*| \cdot \left\| \begin{bmatrix} \Re(\gamma_k) & \Im(\gamma_k) \end{bmatrix}^T - \begin{bmatrix} \Re(d) & \Im(d) \end{bmatrix}^T \right\|_2 \end{aligned} \quad (64)$$

where $d = -\xi_0 / \xi_c^*$. Also,

$$\Im(d) / \Re(d) = \Im(\xi_c) / \Re(\xi_c) = \mathbf{c}_\gamma(2) / \mathbf{c}_\gamma(1). \quad (65)$$

This shows that the origin \mathbf{O} , the center \mathbf{c}_γ and $D = [\Re(d) \ \Im(d)]$ are co-linear on the plane as shown in Fig. 7. Note that in Fig. 7 we have denoted C as the center of the circle. From (64) it can be observed that G_k is a scaling of the Euclidean distance between D and a point $F = [\Re(\gamma_k), \Im(\gamma_k)]^T$ located on the circle \mathcal{C}_γ . From this observation, the optimal solution to (18) can thus be obtained in a geometrical approach below.

Without loss of generality, we first assume that $\Re(d) \neq \mathbf{c}_\gamma(1)$, otherwise, all γ_k on circle \mathcal{C}_k will have the same G_k . In the case of $\Re(d) > \mathbf{c}_\gamma(1) \geq 0$ or $\Re(d) < \mathbf{c}_\gamma(1) < 0$, it can be derived that $\gamma_{k,\star} = \gamma_{k,a}$, i.e., when $F = F_a$, G_k is maximized. In fact, these two cases can be geometrically illustrated by Fig. 7(a) and Fig. 7(b), respectively.

Similarly, in the case of $\mathbf{c}_\gamma(1) \geq 0$, $\Re(d) < \mathbf{c}_\gamma(1)$ (as shown in Fig. 7(c)), or $\mathbf{c}_\gamma(1) < 0$, $\Re(d) > \mathbf{c}_\gamma(1)$ (as shown in Fig. 7(d)), the two points \mathbf{O} and D are located on the same sides (right or left) of C . As a result, $\gamma_{k,\star} = \gamma_{k,b}$, i.e., when $F = F_b$, G_k is maximized in these two cases.

In summary, it can be concluded that if $\zeta > 0$, $\gamma_{k,\star} = \gamma_{k,a}$, otherwise, $\gamma_{k,\star} = \gamma_{k,b}$, where ζ has been defined in (23). This completes the proof.

APPENDIX B PROOF OF PROPOSITION 5

It is easy to see that $-1/\xi_k > \xi_0 / (|\xi_c|^2 - \xi_0 \xi_k)$ in (38) is actually equivalent to

$$(|\xi_c|^2 - \xi_0 \xi_k) \xi_k < 0. \quad (66)$$

When $\mathbf{T}_{k-1} \in \mathbb{S}_{++}^N$, we have $\mathbf{T}_{k-1}^{-1} \in \mathbb{S}_{++}^N$. Thus, from (20b)

$$\xi_k > 0. \quad (67)$$

Let the Cholesky decomposition of \mathbf{T}_{k-1}^{-1} be $\mathbf{T}_{k-1}^{-1} = \mathbf{\Xi} \mathbf{\Xi}^H$, where $\mathbf{\Xi}$ is an invertible matrix. If $\mathbf{a}(\theta_0) \neq \rho \mathbf{a}(\theta_k)$ for $\forall \rho \in \mathbb{C}$ that always holds in array antenna theory, we have $\mathbf{\Xi}^H \mathbf{a}(\theta_0) \neq \rho \mathbf{\Xi}^H \mathbf{a}(\theta_k)$ for $\forall \rho \in \mathbb{C}$. Then, from the Cauchy-Schwarz inequality we have

$$\begin{aligned} |\xi_c|^2 - \xi_0 \xi_k &= |(\mathbf{\Xi}^H \mathbf{a}(\theta_k))^H (\mathbf{\Xi}^H \mathbf{a}(\theta_0))|^2 - \\ &\quad \|\mathbf{\Xi}^H \mathbf{a}(\theta_0)\|_2^2 \cdot \|\mathbf{\Xi}^H \mathbf{a}(\theta_k)\|_2^2 < 0. \end{aligned} \quad (68)$$

Hence, from Proposition 4, we have $\beta_{k,\star} = \beta_{k,r}$.

From (34), (39) and the fact that $\beta_{k,\star} = \beta_{k,r}$, we have

$$\beta_{k,\star} = \frac{|\xi_c| - \sqrt{\rho_k} \xi_0}{\sqrt{\rho_k} (\xi_0 \xi_k - |\xi_c|^2)}. \quad (69)$$

This completes the proof of (44).

Furthermore, if $\mathbf{T}_{k-1} \in \mathbb{S}_{++}^N$, one learns from $\mathbf{T}_k = \mathbf{T}_{k-1} + \beta_{k,\star} \mathbf{a}(\theta_k) \mathbf{a}^H(\theta_k)$ that

$$\mathbf{T}_k \in \mathbb{S}_{++}^N \Leftrightarrow \mathbf{T}_{k-1} + \beta_{k,\star} \mathbf{a}(\theta_k) \mathbf{a}^H(\theta_k) \in \mathbb{S}_{++}^N \quad (70a)$$

$$\Leftrightarrow \mathbf{I} + \beta_{k,\star} \mathbf{T}_{k-1}^{-1/2} \mathbf{a}(\theta_k) \mathbf{a}^H(\theta_k) \mathbf{T}_{k-1}^{-1/2} \in \mathbb{S}_{++}^N \quad (70b)$$

$$\Leftrightarrow 1 + \beta_{k,\star} \mathbf{a}^H(\theta_k) \mathbf{T}_{k-1}^{-1} \mathbf{a}(\theta_k) > 0 \quad (70c)$$

$$\Leftrightarrow \beta_{k,\star} > -1/\xi_k \quad (70d)$$

$$\Leftrightarrow \frac{|\xi_c| \xi_k - \sqrt{\rho_k} |\xi_c|^2}{\sqrt{\rho_k} (\xi_0 \xi_k - |\xi_c|^2) \xi_k} > 0 \quad (70e)$$

$$\Leftrightarrow \rho_k < \xi_k^2 / |\xi_c|^2. \quad (70f)$$

This completes the proof of Proposition 5.

APPENDIX C PROOF OF PROPOSITION 7

From the update procedure of weight vector, one gets

$$\begin{aligned} \mathbf{w}_k &= \mathbf{w}_{k-1} + \gamma_k \mathbf{v}_k \\ &= \mathbf{T}_{k-1}^{-1} \mathbf{a}(\theta_0) - \beta_k \xi_c \mathbf{T}_{k-1}^{-1} \mathbf{a}(\theta_k) / (1 + \beta_k \xi_k). \end{aligned} \quad (71)$$

Then we can obtain $\mathbf{a}^H(\theta_0) \mathbf{w}_k = \xi_0 - \beta_k |\xi_c|^2 / (1 + \beta_k \xi_k)$ and

$$|\mathbf{w}_k^H \mathbf{a}(\theta_0)|^2 = |(\xi_0 \xi_k - |\xi_c|^2) \beta_k + \xi_0|^2 / |1 + \beta_k \xi_k|^2. \quad (72)$$

On the other hand, from (71) we have $\mathbf{w}_k^H \mathbf{T}_{k-1} \mathbf{a} = \mathbf{a}^H(\theta_0) - \beta_k^* \xi_c^* \mathbf{a}^H(\theta_k)/(1 + \beta_k^* \xi_k)$ and further get

$$\begin{aligned} \mathbf{w}_k^H \mathbf{T}_{k-1} \mathbf{w}_k &= (\mathbf{a}^H(\theta_0) - \beta_k^* \xi_c^* \mathbf{a}^H(\theta_k)/(1 + \beta_k^* \xi_k)) \cdot \\ &\quad (\mathbf{T}_{k-1}^{-1} \mathbf{a}(\theta_0) - \beta_k \xi_c \mathbf{T}_{k-1}^{-1} \mathbf{a}(\theta_k)/(1 + \beta_k \xi_k)) \\ &= \frac{(\xi_0 \xi_k - |\xi_c|^2) \xi_k |\beta_k + \frac{1}{\xi_k}|^2 + \frac{|\xi_c|^2}{\xi_k}}{|1 + \beta_k \xi_k|^2}. \end{aligned} \quad (73)$$

Combining (72) and (73), we get

$$\frac{|\mathbf{w}_k^H \mathbf{a}(\theta_0)|^2}{\mathbf{w}_k^H \mathbf{T}_{k-1} \mathbf{w}_k} = \frac{\left(\frac{\xi_0 \xi_k - |\xi_c|^2}{\xi_k}\right) \cdot R_\beta^2}{\left|\beta_k + \frac{1}{\xi_k}\right|^2 + \frac{|\xi_c|^2}{(\xi_0 \xi_k - |\xi_c|^2) \xi_k^2}} \quad (74)$$

where we have utilized the fact that $\xi_0 \xi_k - |\xi_c|^2 > 0$ (see (68) when $\mathbf{T}_{k-1}^{-1} \in \mathbb{S}_{++}^N$) and $|\beta_k + \frac{1}{\xi_k}| = R_\beta$. Obviously, the maximization of $|\mathbf{w}_k^H \mathbf{a}(\theta_0)|^2/(\mathbf{w}_k^H \mathbf{T}_{k-1} \mathbf{w}_k)$ is equivalent to minimizing $|\beta_k + \frac{1}{\xi_k}|$. Define

$$\mathbf{f} \triangleq [-1/\xi_k \quad 0]^T \quad (75)$$

then we can reformulate problem (47) as

$$\underset{\beta_k}{\text{minimize}} \quad \|[\Re(\beta_k) \quad \Im(\beta_k)]^T - \mathbf{f}\|_2 \quad (76a)$$

$$\text{subject to} \quad [\Re(\beta_k) \quad \Im(\beta_k)]^T \in \mathcal{C}_\beta. \quad (76b)$$

On the other hand, substituting the constraint (36c) into G_k and recalling the conclusion of Proposition 3, the array gain satisfies

$$G_k = |\mathbf{a}^H(\theta_0) \mathbf{T}_k^{-1} \mathbf{a}(\theta_0)| \quad (77a)$$

$$= \left| \xi_0 - \frac{\beta_k |\xi_c|^2}{1 + \beta_k \xi_k} \right| \quad (77b)$$

$$= \left| \frac{\xi_0 \xi_k - |\xi_c|^2}{\xi_k} \right| \cdot \left| \frac{\beta_k - \xi_0 / (|\xi_c|^2 - \xi_0 \xi_k)}{\beta_k - (-1/\xi_k)} \right| \quad (77c)$$

$$= \left| \frac{\xi_0 \xi_k - |\xi_c|^2}{\xi_k} \right| \cdot \frac{\|[\Re(\beta_k) \quad \Im(\beta_k)]^T - \mathbf{c}_\beta\|_2}{\|[\Re(\beta_k) \quad \Im(\beta_k)]^T - \mathbf{f}\|_2} \quad (77d)$$

$$= \frac{|\xi_0 \xi_k - |\xi_c|^2| \cdot R_\beta / \xi_k}{\|[\Re(\beta_k) \quad \Im(\beta_k)]^T - \mathbf{f}\|_2}. \quad (77e)$$

Note that (77a) comes from the intermediate result of (19), whereas (77d) is obtained from the result of Proposition 3. Since $|\xi_0 \xi_k - |\xi_c|^2| \cdot R_\beta / \xi_k$ is a constant, from (77e), we can also reformulate problem (36) as (76).

Consequently, if $\mathbf{T}_{k-1} \in \mathbb{S}_{++}^N$, problem (36) has the same optimal solution as the problem (47). This completes the proof.

APPENDIX D DERIVATION OF (52)

We first show

$$\mathbf{T}_{k-1}^{-1} \mathbf{a}(\theta_t) = \mathbf{A}(\theta_t, \theta_{k-1}, \dots, \theta_1) \mathbf{d}_k(\theta_t), \quad \forall \theta_t \in \mathbb{R} \quad (78)$$

where the first component of $\mathbf{d}_k(\theta_t)$ is 1.

We use induction to prove (78). When $k = 1$, since $\mathbf{T}_0 = \mathbf{I}$, (78) is obvious, where $\mathbf{d}_1(\theta_t)$ degenerates to the scalar 1.

Suppose (78) is true when $k = p$, i.e.,

$$\mathbf{T}_{p-1}^{-1} \mathbf{a}(\theta_s) = \mathbf{A}(\theta_s, \theta_{p-1}, \dots, \theta_1) \mathbf{d}_p(\theta_s), \quad \forall \theta_s \in \mathbb{R} \quad (79)$$

where $\mathbf{d}_p(\theta_s)$ is a $p \times 1$ vector with its first entry 1.

When $k = p + 1$, we want to show

$$\mathbf{T}_p^{-1} \mathbf{a}(\theta_r) = \mathbf{A}(\theta_r, \theta_p, \dots, \theta_1) \mathbf{d}_{p+1}(\theta_r), \quad \forall \theta_r \in \mathbb{R} \quad (80)$$

where $\mathbf{d}_{p+1}(\theta_r)$ is a $(p + 1) \times 1$ vector with its first entry 1.

To see (80), one recalls (7) with $k = p$, and (79), and obtains (81) on the top of next page, where

$$\nu = -\beta_p \mathbf{a}^H(\theta_p) \mathbf{T}_{p-1}^{-1} \mathbf{a}(\theta_r) / [1 + \beta_p \mathbf{a}^H(\theta_p) \mathbf{T}_{p-1}^{-1} \mathbf{a}(\theta_p)] \quad (82)$$

$\mathbf{d}_{p+1}(\theta_r)$ is a $(p + 1) \times 1$ vector as shown in (83), where $\mathbf{d}_p(\theta_r)_i$ stands for the i th element of $\mathbf{d}_p(\theta_r)$.

Then, (52) can be seen by substituting (78) with $\theta_t = \theta_k$ into (18c).

APPENDIX E PROOF OF COROLLARY 1

In the first step of the weight vector update in the OPARC, we have $\mathcal{C}_\gamma = \mathcal{C}_\mu$ due to the fact that $\mathbf{T}_0 = \mathbf{I}$ and hence $\mathbf{H}_1 = \mathbf{Q}_1$. Therefore, one gets $\mu_{1,*} = \gamma_{1,a}$ since $[\Re(\gamma_{1,a}) \quad \Im(\gamma_{1,a})]^T$ has the minimum module among the elements in the set \mathcal{C}_γ as shown in Fig. 1.

On the other hand, substituting $\mathbf{v}_1 = \mathbf{a}(\theta_1)$ and $\mathbf{w}_0 = \mathbf{a}(\theta_0)$ into (14) yields $\mathbf{H}_1(1, 2) = (\|\mathbf{a}(\theta_1)\|_2^2 - \rho_1 \|\mathbf{a}(\theta_0)\|_2^2) \cdot \mathbf{a}^H(\theta_0) \mathbf{a}(\theta_1)$ and $\mathbf{H}_1(2, 2) = \|\mathbf{a}(\theta_1)\|_2^4 - \rho_1 |\mathbf{a}^H(\theta_1) \mathbf{a}(\theta_0)|^2$. Recalling (15), we obtain

$$\mathbf{c}_\gamma(1) = \frac{-\Re[\mathbf{a}^H(\theta_0) \mathbf{a}(\theta_1)] (\|\mathbf{a}(\theta_1)\|_2^2 - \rho_1 \|\mathbf{a}(\theta_0)\|_2^2)}{\|\mathbf{a}(\theta_1)\|_2^4 - \rho_1 |\mathbf{a}^H(\theta_1) \mathbf{a}(\theta_0)|^2}.$$

Meanwhile, since $\mathbf{T}_0 = \mathbf{I}$, one obtains from (23) that $\zeta = \text{sign}(\|\mathbf{a}(\theta_1)\|_2^2 - \rho_1 \|\mathbf{a}(\theta_0)\|_2^2)$. Finally, from (22), if $\rho_1 \leq \|\mathbf{a}(\theta_1)\|_2^2 / \|\mathbf{a}(\theta_0)\|_2^2$, we have $\gamma_{1,*} = \gamma_{1,a}$, otherwise, we obtain $\gamma_{1,*} = \gamma_{1,b}$. Recalling $\mu_{1,*} = \gamma_{1,a}$, we complete the proof.

APPENDIX F PROOF OF (55) AND (57)

From the equivalence of (53) and (54), one gets $\mathbf{b}_k = -(\mathbf{I} + \check{\Sigma}_k \mathbf{A}_k^H \mathbf{A}_k)^{-1} \check{\Sigma}_k \mathbf{A}_k^H \mathbf{a}(\theta_0)$. Multiplying by $\mathbf{I} + \check{\Sigma}_k \mathbf{A}_k^H \mathbf{A}_k$ to both sides from the left of this equality yields $\check{\Sigma}_k \mathbf{A}_k^H (\mathbf{a}(\theta_0) + \mathbf{A}_k \mathbf{b}_k) = -\mathbf{b}_k$. Since $\check{\Sigma}_k$ is a diagonal matrix and $\check{\mathbf{w}}_k = \mathbf{a}(\theta_0) + \mathbf{A}_k \mathbf{b}_k$, we obtain

$$\check{\Sigma}_k = \text{Diag}(-\mathbf{b}_k \circ (\mathbf{A}_k^H \check{\mathbf{w}}_k)). \quad (84)$$

Furthermore, as $\mathbf{w}_k = \mathbf{w}_{k-1} + \mu_k \mathbf{a}(\theta_k)$, $\mathbf{b}_k = [\mathbf{b}_{k-1}^T \quad \mu_k]^T$ and $\mathbf{A}_k = [\mathbf{A}_{k-1} \quad \mathbf{a}(\theta_k)]$, we can rewrite (84) as (85) on the top of next page. Consequently, the following formulation can be obtained:

$$\frac{1}{\check{\beta}_{k,i}} = \begin{cases} \frac{1}{\check{\beta}_{k-1,i}} - \frac{\mu_k \mathbf{a}^H(\theta_i) \mathbf{a}(\theta_k)}{\mu_i}, & 1 \leq i \leq k-1 \\ -\frac{\mathbf{a}^H(\theta_k) \check{\mathbf{w}}_{k-1}}{\mu_k} - \|\mathbf{a}(\theta_k)\|_2^2, & i = k. \end{cases} \quad (86)$$

From (86), the powers of interferences can be clearly observed. After some calculation, either (55) or (57) can be derived. This completes the proof.

$$\begin{aligned}\mathbf{T}_p^{-1}\mathbf{a}(\theta_r) &= \mathbf{T}_{p-1}^{-1}\mathbf{a}(\theta_r) + \nu\mathbf{T}_{p-1}^{-1}\mathbf{a}(\theta_p) = \mathbf{A}(\theta_r, \theta_{p-1}, \dots, \theta_1)\mathbf{d}_p(\theta_r) + \nu\mathbf{A}(\theta_p, \theta_{p-1}, \dots, \theta_1)\mathbf{d}_p(\theta_p) \\ &= \mathbf{A}(\theta_r, \theta_p, \dots, \theta_1)\mathbf{d}_{p+1}(\theta_r), \quad \forall \theta_r \in \mathbb{R}\end{aligned}\quad (81)$$

$$\mathbf{d}_{p+1}(\theta_r) = [\mathbf{d}_p(\theta_r)_1, 0, \mathbf{d}_p(\theta_r)_2, \dots, \mathbf{d}_p(\theta_r)_p]^\top + \nu [0, \mathbf{d}_p(\theta_p)_p, \mathbf{d}_p(\theta_r)_{p-1}, \dots, \mathbf{d}_p(\theta_r)_1]^\top \quad (83)$$

$$\begin{aligned}\mathbf{1} \odot \text{diag}(\check{\check{\Sigma}}_k) &= -(\mathbf{A}_{k-1}^H \check{\check{\mathbf{w}}}_k) \odot \mathbf{b}_k = - \begin{bmatrix} \mathbf{A}_{k-1}^H \check{\check{\mathbf{w}}}_k \\ \mathbf{a}^H(\theta_k) \check{\check{\mathbf{w}}}_k \end{bmatrix} \odot \begin{bmatrix} \mathbf{b}_{k-1} \\ \mu_k \end{bmatrix} = - \begin{bmatrix} (\mathbf{A}_{k-1}^H \check{\check{\mathbf{w}}}_{k-1}) \odot \mathbf{b}_{k-1} + (\mu_k \mathbf{A}_{k-1}^H \mathbf{a}(\theta_k)) \odot \mathbf{b}_{k-1} \\ \mathbf{a}^H(\theta_k) \check{\check{\mathbf{w}}}_{k-1} / \mu_k + \|\mathbf{a}(\theta_k)\|_2^2 \end{bmatrix} \\ &= \begin{bmatrix} \mathbf{1} \odot \text{diag}(\check{\check{\Sigma}}_{k-1}) - (\mu_k \mathbf{A}_{k-1}^H \mathbf{a}(\theta_k)) \odot \mathbf{b}_{k-1} \\ -\mathbf{a}^H(\theta_k) \check{\check{\mathbf{w}}}_{k-1} / \mu_k - \|\mathbf{a}(\theta_k)\|_2^2 \end{bmatrix}.\end{aligned}\quad (85)$$

REFERENCES

- [1] R. J. Moulou, *Phased Array Antenna Handbook*. Norwood, MA: Artech House, 1994.
- [2] C. L. Dolph, "A current distribution for broadside arrays which optimizes the relationship between beam width and side-lobe level," *Proc. IRE*, vol. 34, pp. 335-348, 1946.
- [3] K. Chen, X. Yun, Z. He, and C. Han, "Synthesis of sparse planar arrays using modified real genetic algorithm," *IEEE Trans. Antennas Propag.*, vol. 55, pp. 1067-1073, 2007.
- [4] V. Murino, A. Trucco, and C. S. Regazzoni, "Synthesis of unequally spaced arrays by simulated annealing," *IEEE Trans. Signal Process.*, vol. 44, pp. 119-122, 1996.
- [5] D. W. Boeringer and D. H. Werner, "Particle swarm optimization versus genetic algorithms for phased array synthesis," *IEEE Trans. Antennas Propag.*, vol. 52, pp. 771-779, 2004.
- [6] C. A. Olen and R. T. Compton, "A numerical pattern synthesis algorithm for arrays," *IEEE Trans. Antennas Propag.*, vol. 38, pp. 1666-1676, 1990.
- [7] P. Y. Zhou and M. A. Ingram, "Pattern synthesis for arbitrary arrays using an adaptive array method," *IEEE Trans. Antennas Propag.*, vol. 47, pp. 862-869, 1999.
- [8] H. Lebreit and S. Boyd, "Antenna array pattern synthesis via convex optimization," *IEEE Trans. Signal Process.*, vol. 45, pp. 526-532, 1997.
- [9] W. Fan, V. Balakrishnan, P. Y. Zhou, J. J. Chen, R. Yang, and C. Frank, "Optimal array pattern synthesis using semidefinite programming," *IEEE Trans. Signal Process.*, vol. 51, no. 5, pp. 1172-1183, 2003.
- [10] B. Fuchs, "Application of convex relaxation to array synthesis problems," *IEEE Trans. Antennas Propag.*, vol. 62, pp. 634-640, 2014.
- [11] C. Y. Tseng and L. J. Griffiths, "A simple algorithm to achieve desired patterns for arbitrary arrays," *IEEE Trans. Signal Process.*, vol. 40, pp. 2737-2746, 1992.
- [12] W. Stutzman, "Sidelobe control of antenna patterns," *IEEE Trans. Antennas Propag.*, vol. 20, pp. 102-104, 1972.
- [13] J. C. Sureau and K. Keeping, "Sidelobe control in cylindrical arrays," *IEEE Trans. Antennas Propag.*, vol. 30, pp. 1027-1031, 1982.
- [14] T. B. Vu, "Sidelobe control in circular ring array," *IEEE Trans. Antennas Propag.*, vol. 41, pp. 1143-1145, 1993.
- [15] X. Zhang, Z. He, B. Liao, X. Zhang, Z. Cheng, and Y. Lu, "A²RC: an accurate array response control algorithm for pattern synthesis," *IEEE Trans. Signal Process.*, vol. 65, pp. 1810-1824, 2017.
- [16] X. Zhang, Z. He, B. Liao, X. Zhang, and W. Peng, "Pattern synthesis with multipoint accurate array response control," *IEEE Trans. Antennas Propag.*, vol. 65, pp. 4075-4088, 2017.
- [17] H. K. Van Trees, *Optimum Array Processing*. New York: Wiley, 2002.
- [18] L. Griffiths and K. Buckley, "Quiescent pattern control in linearly constrained adaptive arrays," *IEEE Trans. Acoust., Speech, Signal Process.*, vol. 35, pp. 917-926, 1987.
- [19] X. Zhang, Z. He, X.-G. Xia, B. Liao, X. Zhang, and Y. Yang, "OPARC: optimal and precise array response control algorithm – Part II: Multipoints and applications," preprint, Dec. 2017.
- [20] G. H. Golub and C. F. V. Loan, *Matrix Computations*. Baltimore, MD: The Johns Hopkins Univ. Press, 1996.